

# Nonreciprocity in the optical reflection of magnetoplasmas

L. Remer, E. Mohler, W. Grill, and B. Lüthi

*Physikalisches Institut, Universität Frankfurt, D-6000 Frankfurt am Main 1, Germany*

(Received 24 April 1984)

We measured the reflectivity on a slab of  $n$ -type InSb with an incident angle of  $45^\circ$  with different far-infrared laser frequencies of 337-, 311-, and 119- $\mu\text{m}$  wavelengths as a function of applied magnetic field  $B$  between 0 and 10 T. The field was applied in the plane of the surface perpendicular to the reflection plane. We observed clear evidence of nonreciprocal behavior in the reflectivity with respect to field reversal and light-propagation reversal. A simple Drude model accounts satisfactorily for this effect. The influence of damping, crucial for the existence of this effect, is discussed within the framework of electrodynamics as well as with thermodynamic arguments, generalizing Kirchhoff's law of radiation.

## I. INTRODUCTION

Surface excitations exhibit nonreciprocal behavior in the presence of a magnetic field. For a surface in the  $x$ - $y$  plane the frequency of a surface wave  $\omega(k_x, B_y)$  depends on the direction of the wave vector  $\vec{k} = k_x \vec{e}_x$  and on the direction of the magnetic field  $\vec{B} = B_y \vec{e}_y$ , i.e.,  $\omega(k_x, B_y) \neq \omega(-k_x, B_y)$  and  $\omega(k_x, B_y) \neq \omega(k_x, -B_y)$  in general. Such nonreciprocal behavior has been observed for ferromagnetic spin waves,<sup>1</sup> for surface acoustic waves in metals,<sup>2</sup> and for surface polaritons, using the attenuated-total-reflection method.<sup>3,4</sup>

In this paper we show another nonreciprocal effect in the reflection of light on a metal or a semiconductor surface. With application of a magnetic field  $B_y$ , again perpendicular to the plane of incidence [ $(x, z)$  plane], polarized light (with  $\vec{E}$  vector in this plane) shows nonreciprocal behavior (see Fig. 1). We will show that the reflectivity  $R(\alpha)$  is different from  $R(-\alpha)$  with  $\alpha$  the angle of incidence. This also implies  $R(\alpha, B_y) \neq R(\alpha, -B_y)$ . This

effect rests on the same symmetry argument as the one which gives the nonreciprocity of surface excitations mentioned above and which we discuss below.

In the following we first present the theory of the effect, based on a simple application of the Drude model and also generalized to the case of the reflection on a plate of finite thickness. Next, we describe the experiments. Finally, we present the results and a comparison with calculations. We conclude with some remarks based on thermodynamic considerations.

## II. THEORY

We first present the symmetry argument, and then give the theory for the reflection on a half-space plane. We conclude with the calculation of the reflectivity of a thin plate.

### A. Symmetry argument

Although we have discussed the symmetry argument previously,<sup>2</sup> we present it again for completeness. The first presentation was given in a discussion of nonreciprocity of magnetoelastic waves.<sup>5</sup> We consider the same coordinate system as that discussed above and illustrated in Fig. 1. Suppose the crystal possesses mirror symmetry with respect to the  $(x, y)$ ,  $(x, z)$ , and  $(y, z)$  planes. This implies that a reflection operation  $\sigma_{xy}$  leaves the polar vector component  $k_x$  unchanged and changes the axial vector component  $B_y$  into  $-B_y$ . Likewise,

$$\sigma_{yz}(k_x, B_y) = (-k_x, -B_y).$$

This implies that any volume excitation  $\omega(k_x, B_y)$  is even in  $k_x, B_y$ , i.e.,

$$\omega(k_x, B_y) = \omega(k_x, -B_y) = \omega(-k_x, B_y).$$

If we now consider surface excitations, the surface as the  $(x, y)$  plane is no longer a symmetry plane, and therefore, in general,

$$\omega(k_x, B_y) \neq \omega(k_x, -B_y) \text{ and } \omega(k_x, B_y) \neq \omega(-k_x, B_y)$$

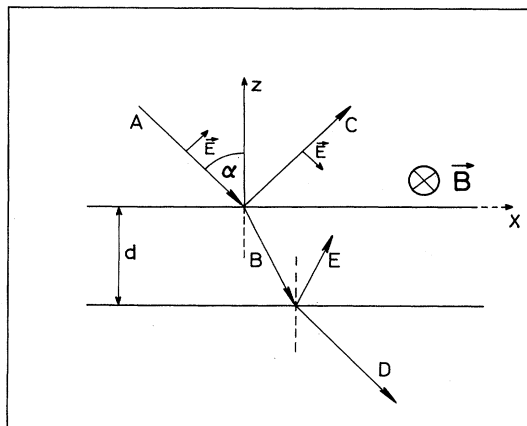


FIG. 1. Schematic plot of the reflection geometry. For the reflection on the half-space only waves A, B, and C are considered.

for any surface excitation. The magnitude of this nonreciprocity depends, of course, on the coupling of the surface excitation to the various magnetic-field-dependent quantities [see, e.g., the discussion of coupling strengths in Ref. 2(b)]. In the case of light reflection on a metal or semiconductor surface, we will show that the nonreciprocity of the light reflection  $R(\alpha) \neq R(-\alpha)$  arises because of the coupling to the nonreciprocal surface-polariton excitations.

### B. Reflection on a half-space

For the calculation of the reflection on a half-space we take a simple Drude dielectric tensor  $\hat{\epsilon}$ . The components  $\epsilon_{ij}$  relevant for the symmetry of Fig. 1 are

$$\epsilon_{xx} = \epsilon_{zz} = \epsilon_0 \left[ 1 - \frac{\omega_p^2 (\omega + i/\tau)}{\omega [(\omega + i/\tau)^2 - \omega_c^2]} \right], \quad (1)$$

$$\epsilon_{xz} = -\epsilon_{zx} = -\epsilon_0 \frac{i\omega_c \omega_p^2}{\omega [(\omega + i/\tau)^2 - \omega_c^2]}.$$

Here,  $\omega_c = eB/m^*c$  is the cyclotron frequency,  $\omega_p = (4\pi ne^2/m^*\epsilon_0)^{1/2}$  is the plasma frequency,  $\epsilon_0$  is the background dielectric constant,  $m^*$  is the effective mass,  $n$  is the density, and  $\tau$  is the relaxation time of the charge carriers.

For the solution of the boundary-value problem one assumes an incident wave  $(E_x^A, E_z^A)$ , a reflected wave  $(E_x^C, E_z^C)$ , and a refracted wave  $(E_x^B, E_z^B)$ . The boundary conditions are

$$E_x^A + E_x^C = E_x^B, \quad E_z^A + E_z^C = E_z^B. \quad (2)$$

These can be written as

$$(1+r)\cos\alpha = E_x^B, \quad (1-r)\sin\alpha = E_z^B, \quad (2')$$

with  $r$  the reflection coefficient, and the amplitude of the incoming wave,  $E^A$ , equal to 1.

The wave equation in the medium ( $z < 0$ ) reads

$$k^2 \vec{E} - \vec{k}(\vec{k} \cdot \vec{E}) = (\omega^2/c^2) \hat{\epsilon} \vec{E}. \quad (3)$$

The wave vector  $\vec{k}$  may be written in the form  $\vec{k} = (\omega/c)(\sin\alpha, 0, \kappa)$ . For the refracted wave, one obtains

$$\kappa = -(\epsilon_v - \sin^2\alpha)^{1/2}, \quad (4)$$

with  $\epsilon_v = \epsilon_{xx} + \epsilon_{xz}^2/\epsilon_{xx}$ . Using  $\text{div} \vec{D} = 0$ , one obtains

$$\sin(\alpha) D_x^B + \kappa D_z^B = 0, \quad (5)$$

which allows to calculate  $D_z^B/E_x^B$  and  $r$ . One finally obtains

$$\frac{1-r}{1+r} = - \frac{\epsilon_{xx}\epsilon_v \cos\alpha}{\epsilon_{xz}\sin\alpha + \epsilon_{xx}\kappa}. \quad (6)$$

A plot of the reflectivity  $R = |r|^2$  is shown in Fig. 2(b) for  $1/\omega_p\tau = 0$  and  $1/\omega_p\tau > 0$  for  $\omega_c/\omega_p = 1.5$ . One notices the following. (1) The reflectivity has two main structures: The plasma edge is shifted to lower frequencies with respect to its  $B=0$  position which is at  $\omega \sim \omega_p$ , and, for higher frequencies, one observes structure at the

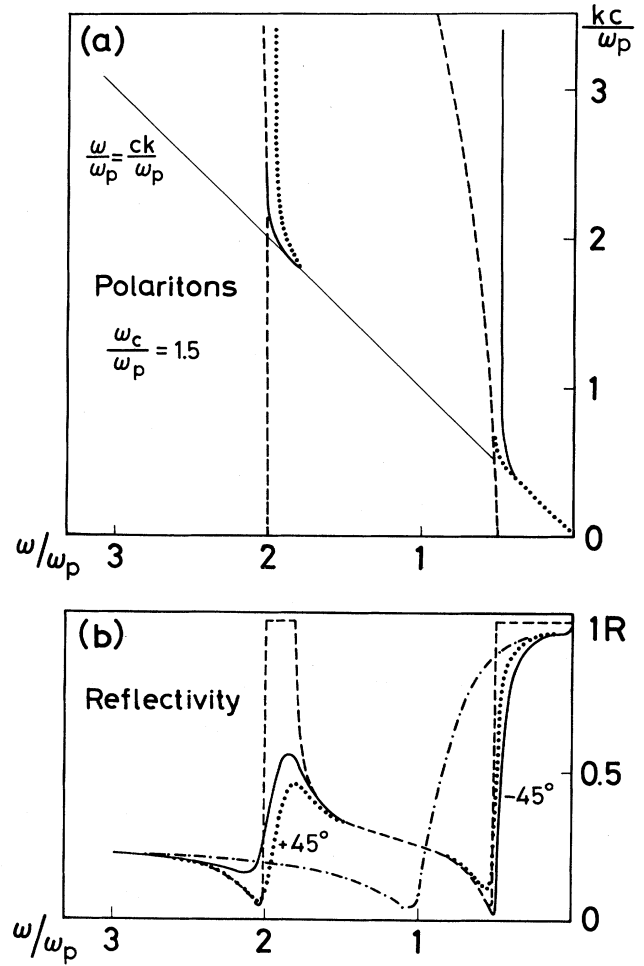


FIG. 2. (a) Calculated dispersion relation for nonreciprocal plasmon polaritons in the presence of a magnetic field  $\omega_c/\omega_p = 1.5$ . (b) Calculated reflectivity for zero magnetic field (dashed-dotted line), for magnetic field  $\omega_c/\omega_p = 1.5$  without damping (dashed line), and for the same magnetic field with damping  $\omega_p\tau = 10$  (solid line,  $\alpha = -45^\circ$ ; dotted line,  $\alpha = +45^\circ$ ).

so-called collective cyclotron resonance. These features are well known and they arise for both cases with damping and no damping. (2) The nonreciprocal behavior arises only for  $1/\omega_p\tau > 0$ , but is absent for  $1/\omega_p\tau = 0$ , i.e., for no damping.

In order to understand these features, in Fig. 2(a) we have plotted the dispersion relations for volume polaritons (dashed lines) and surface polaritons (dotted and solid lines). These calculations were done as discussed elsewhere in full detail<sup>6</sup> and without damping. Comparing Figs. 2(a) and 2(b) with the common axis  $\omega/\omega_p$  shows that the structure in  $R$  is confined to the region where stable surface polaritons exist, and that the nonreciprocal feature in  $R$  is exactly in the same region where the surface polaritons exhibit nonreciprocal features. The existence of stable nonreciprocal surface polaritons leads to nonreciprocal features in the reflectivity  $R$  in the same

frequency region. The fact that the reflectivity  $R$  exhibits nonreciprocal features only for  $1/\omega_p\tau > 0$  is easily explained: In Fig. 2(a) one sees that the thin solid line  $\omega = kc$  does not intersect the surface-polariton branches. Therefore no resonant interaction is possible between the light wave and the surface polaritons. This is the reason for the introduction of the attenuated-total-reflection technique.<sup>7</sup> In the presence of damped surface polaritons, light can couple to the surface polaritons nonresonantly and  $R$  can exhibit the desired effect. In the conclusion we will give, in addition to this kinetic argument, a thermodynamic argument for the necessity of damping for this effect. Formally, the nonreciprocity in  $R$  is due to the term  $\epsilon_{xz}\sin\alpha$  in Eq. (6) which gives the desired function in  $B$  and  $\alpha$ .

### C. Reflection on a plate

Because the damping becomes smaller as one moves away from the plasma edge ( $\omega_c \gg \omega_p$ ), samples with a finite thickness  $d$  become more and more transparent and one observes thickness interferences. We have calculated these by the usual procedures<sup>8</sup> of either summing up the individual reflections or solving the boundary-value problem for the two boundaries. Both methods give the same result; we present the second one here.

The boundary conditions for  $z=0$  and  $z=-d$  are (see Fig. 1 for symbols)

$$\begin{aligned} (1+r')\cos\alpha &= E_x^B + E_x^E, \quad (1-r')\sin\alpha = D_z^B + D_z^E, \\ E_x^B e^{-i\gamma} + E_x^E e^{i\gamma} &= E^D \cos(\alpha) e^{i\delta}, \\ D_z^B e^{-i\gamma} + D_z^E e^{i\gamma} &= E^D \sin(\alpha) e^{i\delta}, \end{aligned} \quad (7)$$

with  $\gamma = (\omega/c)kd$ ,  $\delta = (\omega/c)\cos(\alpha)d$ , and  $r'$  the reflectivity coefficient of the plate.

Two additional equations are obtained from  $\text{div}\vec{D}=0$  for waves  $B$  and  $E$  (note that for wave  $E$  the quantity  $\kappa$  changes sign with respect to wave  $B$ ), namely

$$\sin(\alpha)D_x^B + \kappa D_z^B = 0, \quad \sin(\alpha)D_x^E - \kappa D_z^E = 0. \quad (8)$$

These six equations [Eqs. (7) and (8)] determine the six unknowns,  $r'$ ,  $E^D$ ,  $E_x^B$ ,  $E_z^B$ ,  $E_x^E$ , and  $E_z^E$ . The final result for  $r'$  can be written in the form

$$\frac{1-r'}{1+r'} = \frac{1-r}{1+r} \frac{1+b}{1+a}, \quad (9)$$

where  $r$  is the half-space reflectivity as given by (6), and

$$\begin{aligned} a &= b \frac{\epsilon_{xz}\sin\alpha - \kappa\epsilon_{xx}}{\epsilon_{xz}\sin\alpha + \kappa\epsilon_{xx}}, \\ b &= -e^{-2i\gamma} \frac{\epsilon_{xz}\sin\alpha + \epsilon_{xx}\kappa + \epsilon_{xx}\epsilon_v\cos\alpha}{\epsilon_{xz}\sin\alpha - \epsilon_{xx}\kappa + \epsilon_{xx}\epsilon_v\cos\alpha}. \end{aligned}$$

A typical example of these multiple interferences is shown in Fig. 3 for the parameters given in the figure caption.  $R = |r|^2$  is plotted as a function of the magnetic field  $B$  for  $n$ -type InSb. One notices nonreciprocal behavior near the plasma edge where the calculation coincides with the calculation of the half-plane case, but

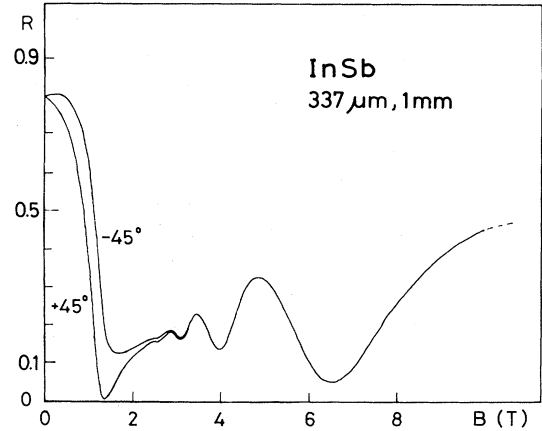


FIG. 3. Calculated reflectivity for a plate 1 mm thick, wavelength 337  $\mu\text{m}$  ( $\omega/\omega_p = 0.525$ ),  $\omega_p\tau = 5$ , and  $\alpha = \pm 45^\circ$ .

strictly reciprocal behavior for  $|\omega_c/\omega_p| \gg 1$ . This is clear by looking again at Fig. 2(a). For  $|\omega_c/\omega_p| \gg 1$  there are no longer any surface polaritons to couple at  $\omega/\omega_p$  fixed. The two polariton branches move further away from  $\omega/\omega_p$ .

### III. EXPERIMENT

The reflection measurements were performed on an  $n$ -type InSb sample using a superconducting magnet. The sample temperature was stabilized at 80 K. For guiding the laser light we used 10-mm-diam stainless-steel tubes. The use of light pipes offers the possibility of easily changing the direction of the light path. The reflected intensity was detected outside the magnet by a room-temperature Golay cell. The grid polarizers were placed near the sample in order to obtain maximum accuracy of polarization. The electromagnetic radiation at 119  $\mu\text{m}$  was generated by a commercially available infrared-pumped far-infrared laser. Modulation was achieved by electrically chopping the pump power (20 Hz). The 337- and 311- $\mu\text{m}$  radiation was generated by a mechanically chopped cw HCN laser. The average power obtained was a few milliwatts.

The theoretical curves, shown in Figs. 4–6, are based on the material parameters given in the literature,<sup>9</sup> with minor corrections in order to optimize the agreement between the theoretical calculations and the experimental data. The InSb crystal was tellurium-doped ( $n$  type) with a nominal concentration of  $n = 1 \times 10^{16}/\text{cm}^3$ . The actual parameters used for the calculations are the following:  $n = 8 \times 10^{15}/\text{cm}^3$ ,  $m^* = 0.015m_0$ ,  $\epsilon_0 = 15$ ,  $\omega_p = 10.64 \times 10^{12} \text{ s}^{-1}$ , and  $\omega_p\tau = 5$ .

### IV. RESULTS AND DISCUSSION

In Figs. 4–6 we show the reflectivity  $R$  as a function of applied field for various laser frequencies. For the wavelengths 337 and 311  $\mu\text{m}$  the corresponding frequencies are below the zero-field plasma frequency of the material.

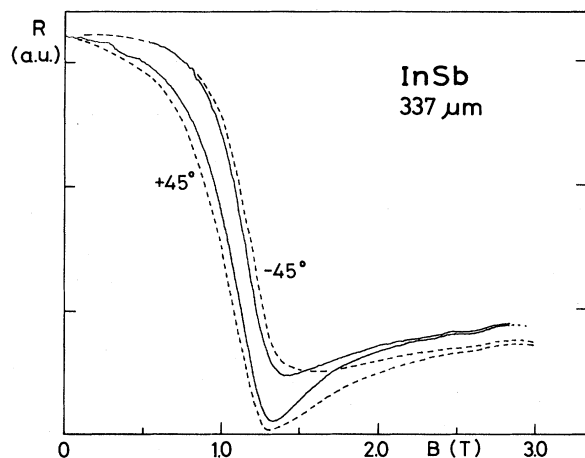


FIG. 4. Measured reflectivity  $R$  (arbitrary units) vs magnetic field  $B$  for  $n$ -type InSb.  $\lambda = 337 \mu\text{m}$  (solid lines), dashed lines calculated with parameters given in the text ( $\omega/\omega_p = 0.525$ ), and  $T = 80 \text{ K}$ .

For the  $119\text{-}\mu\text{m}$  line the laser frequency is above the zero-field  $\omega_p$  value [see Fig. 2(b)]. Therefore the results for  $337$  and  $311 \mu\text{m}$  give a field dependence of the reflectivity characteristic for  $\omega$  near the plasma edge, and the  $119\text{-}\mu\text{m}$  line exhibits features characteristic for  $\omega$  close to the collective cyclotron frequency. The solid lines in the three figures give the recorder tracings of the reflectivity for the three wavelengths, and the dashed lines give calculated curves using Eqs. (6) and (9). For this fit we used, in all three figures, the same material parameters as given in the preceding section.

The agreement between experiment and theory is very good. The nonreciprocal effect is clearly seen for all three wavelengths. The results of Fig. 4 were measured by interchanging the magnetic field or the angle of incidence, whereas the results of Figs. 5 and 6 were measured only by changing  $B$  to  $-B$  for technical reasons. The remaining small discrepancies between the experimental results

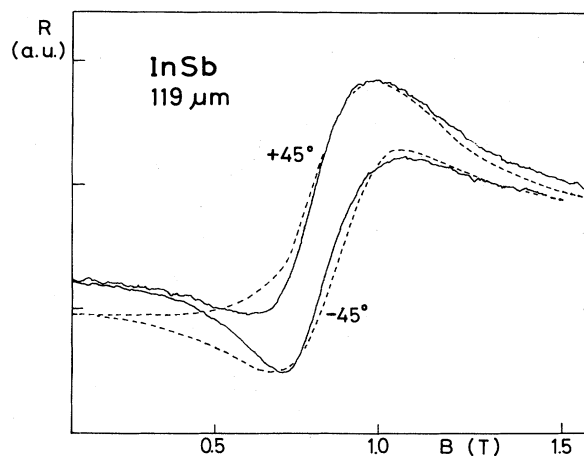


FIG. 6. Measured and calculated reflectivity for  $\lambda = 119 \mu\text{m}$ , same symbols as in Fig. 4 ( $\omega/\omega_p = 1.488$ ), and  $T = 80 \text{ K}$ .

and the calculations can be traced to both experimental and theoretical inadequacies. Experimentally, the use of polarizers with an imperfect degree of polarization changes the overall reflectivity. Theoretically, the use of an isotropic Drude model with a single effective mass and a frequency-independent  $\epsilon_0$  can, at best, be semiquantitatively correct. Since we are only interested in exhibiting the nonreciprocal features in the reflectivity and accounting for it theoretically, and since we do not want to determine material parameters with this experiment, we do not present more elaborate calculations. In Ref. 4 reflection results similar to ours for  $337 \mu\text{m}$  were presented at microwave frequencies.

Finally, in Fig. 7 we show the reflectivity  $R$  for a larger field range from  $0$  to  $10 \text{ T}$  for  $\lambda = 337 \mu\text{m}$ . We observe the thickness interferences for fields larger than  $2 \text{ T}$ . For these fields the effect is reciprocal within the accuracy of our experiment, and the effect agrees qualitatively with the theoretical curve of Fig. 3. Again, we do not attempt

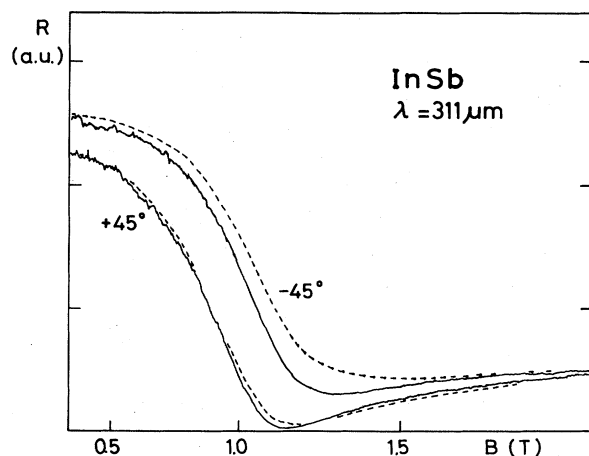


FIG. 5. Measured and calculated reflectivity for  $\lambda = 311 \mu\text{m}$ , same symbols as in Fig. 4 ( $\omega/\omega_p = 0.570$ ), and  $T = 80 \text{ K}$ .

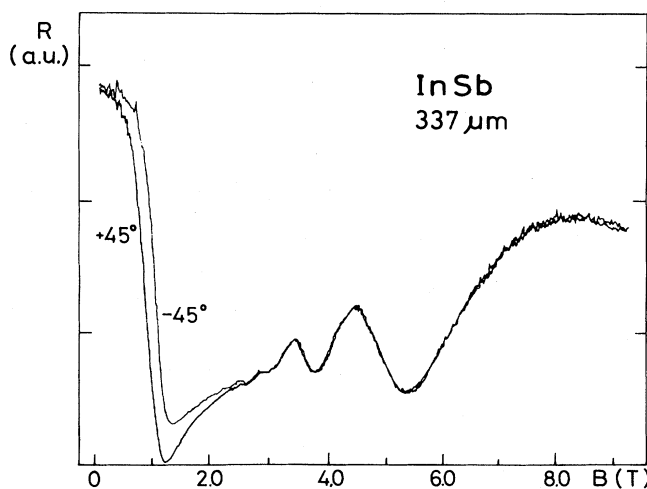


FIG. 7. Measured reflectivity for  $\lambda = 337 \mu\text{m}$  exhibiting thickness interferences for a  $1\text{-mm}$ -thick InSb plate;  $T = 80 \text{ K}$ .

to fit the curve exactly by changing the parameters  $\gamma$ , etc., the reason being that the calculation is made for an infinite plate, whereas one has to use a finite plate for realistic calculations. However, the salient features of the thickness-interference effect as observed in Fig. 7 are clearly exhibited in Fig. 3.

## V. CONCLUSIONS

In the preceding sections we have given a detailed presentation of the experimental results and the calculation of the nonreciprocal effect in the light reflectivity of a metal surface. Such an effect was proposed before for magnetic media, where it was called equatorial Kerr effect.<sup>10</sup> A presentation of an analogous treatment involving surface spin waves for ferromagnets and antiferromagnets will be presented elsewhere. Here we would like to conclude with a thermodynamic argument which emphasizes the necessity of absorption effects in the metal for the existence of nonreciprocity, and which sheds light on analogous effects in the emissivity and absorptivity as well as generalizing Kirchhoff's law of radiation.

We outline the thermodynamical treatment of the problem as follows. For a given material we define the emittance  $E(\alpha, \phi, \omega, T)$  as the power of an electromagnetic wave of frequency  $\omega$  within a frequency interval  $d\omega$  being radiated into a direction  $(\alpha, \phi)$  within a solid angle  $d\Omega$  across a surface element  $dF$  of the material at the temperature  $T$  divided by the power of an electromagnetic wave radiated under the same conditions from a black-body radiator. Here,  $\alpha$  was defined in Sec. II and  $\phi$  is the angle of the reflection plane with respect to the magnetic field. The absorptance  $A(\alpha, \phi, \omega, T)$ , the transmittance  $T(\alpha, \phi, \omega, T)$ , and the reflectance  $R(\alpha, \phi, \omega, T)$  are defined in the usual way, with  $(\alpha, \phi)$  defined for the incident wave.

For a homogeneous material at temperature  $T$  filling a half-space, and the radiation exchanged through a surface element  $\Delta F$  with a black-body radiator at the same temperature under angles  $\alpha$  and  $-\alpha$ , conservation of energy and detailed balance lead to

$$A(\alpha) + R(\alpha) = A(-\alpha) + R(-\alpha) = 1.$$

Therefore a nonreciprocal reflection can only be present if

$$A(\alpha) \neq A(-\alpha),$$

and it disappears if  $A(\alpha)$  or  $A(-\alpha)$  approach zero. The second law of thermodynamics demands that

$$R(\alpha) + E(-\alpha) = R(-\alpha) + E(\alpha) = 1.$$

Otherwise, starting from thermal equilibrium, a temperature difference between the material and the black-body radiator could build up. It follows that  $E(\alpha) = A(-\alpha)$ , and for a nonreciprocal reflectivity  $R(\alpha) \neq R(-\alpha)$  it follows that  $E(\alpha) \neq E(-\alpha)$ . In this case  $E(\alpha) \neq A(\alpha)$ , and Kirchhoff's law, which for our definition of  $E$  and  $A$  can be written as  $E = A$  for all materials, has to be generalized in the presence of nonreciprocal reflection to  $E(\alpha) = A(-\alpha)$  for any  $\alpha, \phi, \omega$ , temperature, and material. We would like to point out that Kirchhoff himself has already stated that his result  $E(\alpha) = A(\alpha)$  (in our notation) is de-

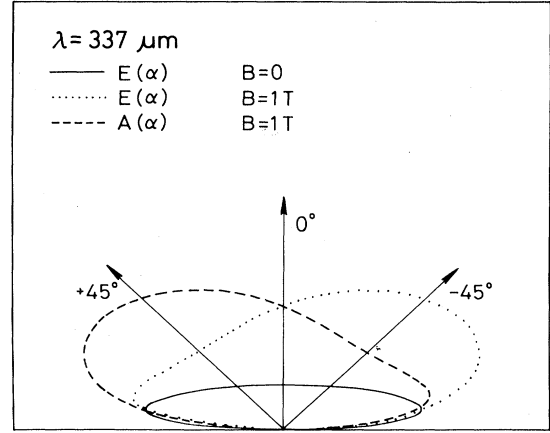


FIG. 8. Calculated absorptance and emittance for  $\lambda = 337 \mu\text{m}$  and same parameters as before for  $B = 0$  and 1 T in polar coordinates for a plate 1 mm thick.

rived in the absence of magnetic fields which, in our application, are the origin of the nonreciprocal reflection.<sup>11</sup> Figure 8 shows an example of the nonreciprocal absorptance and emittance as calculated by electrodynamics and the generalized Kirchhoff's law.

We now discuss the case of a plane parallel plate of finite thickness of homogeneous material with a transmission  $T(\alpha) \neq 0$ . We consider the case of an extended black-body radiator at the same temperature on each side of this plate.

We observe the radiation being exchanged between the plate and the black-body radiators through a surface element on one side of the plate. Detailed balance, the second law of thermodynamics, and the inversion symmetry of the problem demand that (absorbed power equals emitted power)

$$A(\alpha) + A(-\alpha) = E(\alpha) + E(-\alpha).$$

Under thermal equilibrium the material of the plate being penetrated by the observed radiation should not start to rotate if separated from the rest of the material due to the transfer of momentum by the absorbed and emitted radiation; therefore,

$$A(\alpha) - A(-\alpha) = E(-\alpha) - E(\alpha).$$

This again leads to  $E(\alpha) = A(-\alpha)$ . From conservation of energy we further derive  $A(\alpha) + R(\alpha) + T(\alpha) = 1$ , and from the second law of thermodynamics,  $E(-\alpha) + R(\alpha) + T(-\alpha) = 1$ . This yields  $T(\alpha) = T(-\alpha)$  even for  $R(\alpha) \neq R(-\alpha)$ , which proves that even with the reflectivity being nonreciprocal the transmission will always be reciprocal.

This thermodynamical treatment, assuming only the presence of nonreciprocal reflectivity, is in full agreement with the calculations based on electrodynamics given in Sec. II and leads to a generalized Kirchhoff's law for this

case. We have shown by explicit electrodynamic calculations and by this thermodynamical argument that nonreciprocal reflection can only occur in the presence of (nonreciprocal) absorption. The experimental proof of this generalized Kirchhoff's law [ $E(\alpha) = A(-\alpha)$ ] and of the reciprocal transmission in the presence of nonreciprocal reflectivity remains to be demonstrated.

#### ACKNOWLEDGMENTS

We would like to thank Dr. Brazis, Vilnius, and Dr. Pisarev, Leningrad, for drawing our attention to Refs. 4 and 10. This work was supported by the Deutsche Forschungsgemeinschaft (under Sonderforschungsbereich 65, Frankfurt-Darmstadt, West Germany).

---

<sup>1</sup>P. Grünberg and F. Metawe, Phys. Rev. Lett. **39**, 1561 (1977).

<sup>2</sup>(a) J. Heil, B. Lüthi, and P. Thalmeier, Phys. Rev. B **25**, 6515 (1982); (b) J. Phys. C (to be published).

<sup>3</sup>A. Hartstein and E. Burstein, Solid State Commun. **14**, 1223 (1974); A. Hartstein, E. Burstein, E. D. Palik, R. W. Gammon, and B. W. Hennis, Phys. Rev. B **12**, 3186 (1975).

<sup>4</sup>V. S. Ambrazeviciene and R. S. Brazis, Solid State Commun. **18**, 415 (1976).

<sup>5</sup>R. Q. Scott and D. L. Mills, Phys. Rev. B **15**, 3545 (1977).

<sup>6</sup>R. F. Wallis, J. J. Brion, E. Burstein, and A. Hartstein, Phys. Rev. B **9**, 3424 (1974).

<sup>7</sup>A. Otto, Z. Phys. **216**, 398 (1968).

<sup>8</sup>A. Sommerfeld, *Optik, Vorlesungen über Theoretische Physik* (Akademische Verlagsgesellschaft, Leipzig, 1959).

<sup>9</sup>*Landolt-Börnstein Zahlenwerte und Funktionen*, edited by K.-H. Hellwege (Springer, Berlin, 1982), Group III, Vol. 17a, pp. 310–327.

<sup>10</sup>See, e.g., P. S. Pershan, J. Appl. Phys. **38**, 1482 (1967), and references therein.

<sup>11</sup>G. Kirchhoff, reprinted in *Abhandlungen über Emission und Absorption*, edited by M. Planck (Akademische, Verlagsgesellschaft, Leipzig, 1921).